Magneto-acoustic effect in n-InSb at low temperatures

1986 J. Phys. C: Solid State Phys. 19 1431

(http://iopscience.iop.org/0022-3719/19/9/013)

J. Phys. C: Solid State Phys. **19** (1986) 1431–1441. Printed in Great Britain

Magneto-acoustic effect in n-InSb at low temperatures

Chhi-Chong Wu† and Jensan Tsai‡

† Institute of Electronics, National Chiao Tung University, Hsinchu, Taiwan, China

‡ Institute of Nuclear Science, National Tsing Hua University, Hsinchu, Taiwan, China

Received 5 February 1985, in final form 29 April 1985

Abstract. Using the velocity operator derived from the Heisenberg equation of motion, we have investigated the magneto-acoustic effect in n-InSb in the presence of a DC magnetic field $\boldsymbol{B}$ directed along the propagation of acoustic waves. Since we are interested in both high and low frequency regions, an electron relaxation time due to the scatterings in solids is taken into account. It is found that there exists a discontinuous point in the absorption coefficient or change in the sound velocity as a function of the sound frequency. When the sound frequency is below 1.3×10^{11} rad s^{-1}, the absorption coefficient increases with the sound frequency and the sound velocity decreases with the sound frequency from the sound velocity $v_s = 4 \times 10^5$ cm s^{-1}. However, when the sound frequency is over 1.3×10^{11} rad s^{-1}, the absorption coefficient decreases with the sound frequency and the sound velocity increases abruptly with the sound frequency from $v_s = 4 \times 10^5$ cm s^{-1}.

1. Introduction

Quantum effects have been investigated intensively in such semiconductors as indium antimonide (Frederikse and Hosler 1957, Broom 1958, Aliev *et al* 1975) because of the high carrier mobilities and small effective masses in this compound. When the acoustic wave is propagating parallel to a DC magnetic field, the effect of non-parabolicity and quantum effects will appear much more important in the high-magnetic-field region (Wu and Tsai 1972, Sharma and Phadke 1972, Sutherland and Spector 1978). These magneto-acoustic phenomena in semiconductors are dominated by the linear longitudinal conductivity, because the longitudinal field is important when the interaction of acoustic waves with the conduction electrons in semiconductors is either by piezo-electric or deformation-potential coupling (Spector 1966). Sutherland and Spector (1978) have derived the effective longitudinal conductivity tensor including the phenomena of conduction and diffusion to study magneto-acoustic effects in n-InSb. They have taken into account the non-parabolicity of energy bands and the electron relaxation time for the longitudinal and transverse configurations. Their results have revealed that the non-parabolicity of the energy bands leads to an enhancement of the magneto-acoustic absorption with increasing DC magnetic field, while the relaxation time leads to a decrease in the absorption coefficient with the field. However, experimental results have indicated that the piezo-electric scattering is predominantly responsible for the electron energy relaxation and that the deformation-potential scattering appears to play no significant role in the electron energy relaxation (Lifshitz *et al* 1966, Whalen and Westgate 1972). In our previous work for acoustic waves propagating at an angle θ relative to the direction

of a DC magnetic field $\boldsymbol{B}$ in non-degenerate semiconductors (Wu and Tsai 1979), it has been shown that variation in the direction of the magnetic field with respect to the direction of propagation of acoustic waves will affect the acoustic absorption coefficient and change the sound velocity. The result is in qualitative agreement with experimental results (Smith *et al* 1971) in which the deformation potential and piezo-electric attenuation had been investigated separately. In those works, since we are interested in the high-frequency region such that $|\boldsymbol{q}|l \gg 1$, where $\boldsymbol{q}$ is the acoustic wave-vector and l is the electron mean free path, the effect of scattering can be neglected and we did not take into account the effect of the electron relaxation time. However, when we are also interested in the low-frequency region, the effect of scattering cannot be neglected in real crystals, because there are sufficient imperfections to provide plenty of scatterings even at low temperatures. Hansen (1981) proposed a correct form of the velocity operator from the Hamiltonian operator to show that the Hall effect is not influenced by non-parabolicity in the limit of vanishing scattering. In our present work, we shall study the quantum effect on the longitudinal magneto-acoustic phenomena in non-degenerate semiconductors such as n-InSb by taking into account the effect of an electron relaxation time due to the scattering in solids. We use the Heisenberg equation of motion to correct the non-linear effect of the energy band structure in semiconductors. We also make the following assumptions:

(i) For a non-degenerate semiconductor, the distribution function of electrons is represented by the Maxwell–Boltzmann distribution.

(ii) As we are interested in both the high- and low-frequency regions, the effect of scatterings cannot be neglected. Hence we take into account the effect of electron relaxation time in our calculations.

(iii) The energy band structure is assumed to be non-parabolic.

(iv) The interaction between the conduction electrons and acoustic waves in semiconductors occurs by means of deformation-potential and piezo-electric couplings.

Experiments with acoustic phonons in the frequency range from 10^{10} Hz up to the maximum lattice frequency of about 10^{13} Hz yield information on acoustic wave propagation and scattering. In experiments (Grill and Weiss 1974) phonon pulses in quartz have been generated at 891 GHz using piezo-electric surface excitation by use of a molecular laser. In our present study, we shall investigate the magneto-acoustic phenomena in semiconductors up to 160 GHz (approximately 10^{12} rad s^{-1}).

In § 2, we perform the calculation of the linear longitudinal conductivity for a non-parabolic band structure in the presence of a DC magnetic field $\boldsymbol{B}$ by introducing an electron relaxation time. In § 3, some numerical results for n-InSb are presented. Finally, we discuss these numerical results in § 4.

2. Quantum treatment of the linear longitudinal conductivity

In the non-parabolic model, the energy eigenvalue equation for electrons in a uniform DC magnetic field $\boldsymbol{B}$ directed along the z axis is

$$H_0\left(1+\frac{H_0}{E_g}\right)\Psi_{kn}=\left(\frac{1}{2m^*}\right)\left[p_x^2+\left(p_y-\frac{eBx}{c}\right)^2+p_z^2\right]\Psi_{kn}=E_{kn}\left(1+\frac{E_{kn}}{E_g}\right)\Psi_{kn} \qquad (1)$$

where m^* is the effective mass of electrons at the minimum of the conduction band, E_g is the energy gap between the conduction and valence bands, and E_{kn} is the true energy

of the system defined by $H_0\Psi_{kn} = E_{kn}\Psi_{kn}$. In equation (1) we have used the Landau gauge for the vector potential $\boldsymbol{A}_0 = (0, Bx, 0)$. The eigenfunctions and eigenvalues for equation (1) can be expressed as

$$\Psi_{kn} = \exp(ik_y y + ik_z z)\varphi_n[x - (\hbar c/eB)k_y] \tag{2}$$

and

$$E_{kn} = -\tfrac{1}{2}E_g[\![1 - \{1 + (4/E_g)[(n + \tfrac{1}{2})\hbar\omega_c + \hbar^2 k_z^2/2m^*]\}^{1/2}]\!] \tag{3}$$

where k_y and k_z are the y and z components of the electron wave-vector $\boldsymbol{k}$, $\varphi_n(x)$ is the harmonic-oscillator wavefunction, and $\omega_c = |e|B/m^*c$ is the cyclotron frequency of electrons.

The interaction of conduction electrons with acoustic waves can be taken into account using the vector potential $\boldsymbol{A}_1 = \boldsymbol{A}_{10}\exp(i\boldsymbol{q}\cdot\boldsymbol{r} - i\omega t)$, which arises from the self-consistent field accompanying acoustic waves. In the present case, we are interested in acoustic waves propagating parallel to the DC magnetic field. The current density $\boldsymbol{J}$ can be obtained by taking the trace of the density matrix $\boldsymbol{\rho}$ and the current density operator $\boldsymbol{J}_{op}$ (Smith 1969, Nag 1972)

$$\boldsymbol{J} = \mathrm{Tr}(\boldsymbol{\rho}\cdot\boldsymbol{J}_{op}) = \sum_{kk',nn'} \langle k'n'|\boldsymbol{\rho}|kn\rangle\langle kn|\boldsymbol{J}_{op}|k'n'\rangle. \tag{4}$$

Here the current density operator $\boldsymbol{J}_{op}$ induced by the self-consistent field at a point $\boldsymbol{r}_0$ is

$$\boldsymbol{J}_{op} = \left[\frac{e}{2}\boldsymbol{v} - \frac{e\boldsymbol{A}_1}{m^*c}\Big/\left(1 + \frac{H_0^{(r)}}{E_g} + \frac{H_0^{(l)}}{E_g}\right), \delta(\boldsymbol{r} - \boldsymbol{r}_0)\right]_+ \tag{5}$$

where $[\ ,\ ]_+$ is the anti-commutator bracket, $H_0^{(r)}$ and $H_0^{(l)}$ are the right and left Hamiltonian operators, such that

$$H_0^{(r)}\Psi_{kn} = E_{kn}\Psi_{kn} \tag{6}$$

and

$$\Psi_{k'n'}^* H_0^{(l)} = E_{k'n'}\Psi_{k'n'}^* \tag{7}$$

respectively, and the velocity operator $\boldsymbol{v}$ can be obtained from the Heisenberg equation of motion,

$$\boldsymbol{v} = (1/i\hbar)[\boldsymbol{r}, H_0] \tag{8}$$

where $[\ ,\ ]$ is the commutator bracket. The density matrix $\boldsymbol{\rho}$ should satisfy the quantum Liouville equation (Sutherland and Spector 1978)

$$\frac{\partial\boldsymbol{\rho}}{\partial t} + \frac{i}{\hbar}[H, \boldsymbol{\rho}] = -(\boldsymbol{\rho} - \boldsymbol{\rho}_s)/\tau \tag{9}$$

where

$$H = H_0 + H_1 \tag{10}$$

with

$$H_1 = -(e/2c)(\boldsymbol{v}\cdot\boldsymbol{A}_1 + \boldsymbol{A}_1\cdot\boldsymbol{v}). \tag{11}$$

τ is the electron relaxation time due to the scattering in solids and $\boldsymbol{\rho}_s$ is the appropriate equilibrium density matrix. Using the gauge where the scalar potential is zero, the

relation between the electric field and the vector potential is given by

$$\boldsymbol{E} = (\mathrm{i}\omega/c)\boldsymbol{A}_1. \tag{12}$$

From equations (4), (5), (8) and (9), the current density $\boldsymbol{J}$ can be expressed by

$$\boldsymbol{J} = \boldsymbol{\sigma} \cdot \boldsymbol{E} \tag{13}$$

where $\boldsymbol{\sigma}$ is the linear conductivity tensor. The linear longitudinal conductivity can be obtained as

$$\sigma_{zz}(\boldsymbol{q}, \omega) = \frac{\omega_{\mathrm{p}}^{*2}}{4\pi \mathrm{i}\omega n_0}\left(\sum_{k,n} f_{kn}\Theta_{kn} - (\hbar^2/4m^*)\sum_{k,n}(\Theta_{k+qn}^{kn})^2(2k_z + q_z)^2 \right.$$
$$\left. \times \frac{(f_{kn} - f_{k+qn})}{E_{k+qn} - E_{kn} - \hbar(\omega + \mathrm{i}\tau^{-1})}\right) \tag{14}$$

where $\omega_{\mathrm{p}}^* = (4\pi n_0 e^2/m^*)^{1/2}$ is the plasma frequency, n_0 is the electron density of materials, and f_{kn} is the Maxwell–Boltzmann distribution since we have assumed a non-degenerate semiconductor. Functions Θ_{kn} and $\Theta_{k'n'}^{kn}$ are defined by

$$\Theta_{kn} = (1 + 2E_{kn}/E_{\mathrm{g}})^{-1} \tag{15}$$

and

$$\Theta_{k'n'}^{kn} = \left(1 + \frac{E_{kn}}{E_{\mathrm{g}}} + \frac{E_{k'n'}}{E_{\mathrm{g}}}\right)^{-1} \tag{16}$$

respectively.

From equation (14), it can be seen that the factor $\Theta_{k'n'}^{kn}$ defined by equation (16) appears with the second-degree term of this factor in the linear conductivity σ_{zz} instead of Θ_{kn} defined by equation (15) as shown in our previous work (Wu and Tsai 1979). This correction is made from the velocity operator $\boldsymbol{v}$ given by equation (8).

3. Numerical analysis

Since $(\hbar k_{z\max})^2/2m^* \simeq k_{\mathrm{B}}T \ll E_{\mathrm{g}}$ at low temperatures ($T < 100$ K) in which we are interested, equation (3) can be expanded as

$$E_{kn} \simeq -\tfrac{1}{2}E_{\mathrm{g}} + \tfrac{1}{2}E_{\mathrm{g}}a_n + \hbar^2 k_z^2/2m^* a_n \tag{17}$$

with

$$a_n = [1 + (4\hbar\omega_{\mathrm{c}}/E_{\mathrm{g}})(n + \tfrac{1}{2})]^{1/2}. \tag{18}$$

That is, the factor a_n will play an important role in the non-parabolic band structure at low temperatures and strong magnetic fields. Equation (14) becomes as

$$\sigma_{zz} = \frac{(\omega_{\mathrm{p}}^*)^2(\theta E_{\mathrm{g}})^{1/2}}{4(2\pi)^{1/2}\mathrm{i}\omega\sum_n a_n^{1/2}\exp(-\frac{1}{2}E_{\mathrm{g}}\theta a_n)}\left[\left[\sum_n \exp(-\tfrac{1}{2}E_{\mathrm{g}}\theta a_n)\, W[\mathrm{i}(\tfrac{1}{2}E_{\mathrm{g}}\theta a_n)^{1/2}]\right.\right.$$
$$- \frac{q_\hbar E_{\mathrm{g}}^{3/2}}{4(m^*)^{1/2}}\sum_n \exp(-\tfrac{1}{2}E_{\mathrm{g}}\theta a_n)(A_{nq})^{-1}\left\{\left[\frac{q\hbar\theta}{m^*}(\tfrac{1}{4}q^2\hbar^2 + m^* E_{\mathrm{g}}a_n^2)^{1/2}\right.\right.$$
$$\left.\left. + \mathrm{i}\left(\frac{q^2\hbar^2\theta}{2m^*} + 2a_n(2 + E_{\mathrm{g}}\theta a_n) - 4q^2\hbar^2(\tfrac{1}{4}q^2\hbar^2\right.\right.\right.$$

$$+ m^* E_g a_n^2)/(m^{*2} a_n A_{nq})\Big)\Big]$$

$$\times W\{(\theta/2m^* a_n)^{1/2}[\tfrac{1}{2}q\hbar + \mathrm{i}(\tfrac{1}{4}q^2\hbar^2 + m^* E_g a_n^2)^{1/2}]\}$$

$$+ \Big[\frac{q\hbar\theta}{m^*}(\tfrac{1}{4}q^2\hbar^2 + m^* E_g a_n^2)^{1/2} - \mathrm{i}\Big(\frac{q^2\hbar^2\theta}{2m^*} + 2a_n(2 + E_g\theta a_n)$$

$$- 4q^2\hbar^2(\tfrac{1}{4}q^2\hbar^2 + m^* E_g a_n^2)/(m^* a_n A_{nq})\Big)\Big]$$

$$\times W\{-(\theta/2m^* a_n)^{1/2}[\tfrac{1}{2}q\hbar - \mathrm{i}(\tfrac{1}{4}q^2\hbar^2 + m^* E_g a_n^2)^{1/2}]\}$$

$$+ \frac{4\mathrm{i}\Omega^2\hbar^2 a_n}{A_{nq}}\Big\{W\Big[(\theta/2m^* a_n)^{1/2}\Big(\tfrac{1}{2}q\hbar + \frac{\Omega m^* a_n}{q}\Big)\Big]$$

$$- W\Big[-(\theta/2m^* a_n)^{1/2}\Big(\tfrac{1}{2}q\hbar - \frac{\Omega m^* a_n}{q}\Big)\Big]\Big\}\Big] \tag{19}$$

where $\theta = 1/k_B T$, $\omega_c = |e|B/m^* c$, $\Omega = \omega + \mathrm{i}\tau^{-1}$, the function $W(z) = \exp(-z^2)\,\mathrm{erfc}(-\mathrm{i}z)$ is a function related to the complementary error function (Abramowitz and Stegun 1964), and

$$A_{nq} = \Omega^2\hbar^2 + E_g q^2\hbar^2/m^* + (q^2\hbar^2/2m^* a_n)^2. \tag{20}$$

It has been assumed that the interaction between the conduction electrons and acoustic waves in semiconductors occurs through deformation-potential and piezo-electric couplings. The piezo-electric coupling is the dominant interaction for frequencies in or below the microwave region. At frequencies above the microwave region, the deformation-potential coupling becomes dominant owing to its stronger frequency dependence (Spector 1966). The relation between the absorption coefficient $\alpha_\parallel$ and the longitudinal conductivity σ_{zz} is thus given by (Abe and Mikoshiba 1971)

$$\alpha_\parallel = -(4\pi q/d\varepsilon v_s^2)[\beta^2 + (C\omega\varepsilon/4\pi e v_s)^2]\,\mathrm{Im}[1 - (4\pi\sigma_{zz}/\mathrm{i}\omega\varepsilon)]^{-1} \tag{21}$$

where d is the density of the material, ε is the static dielectric constant, v_s is the sound velocity, β is an appropriate piezo-electric constant, and C is the deformation potential. For $\boldsymbol{q}$ parallel to the [110] direction $\beta = \beta_{14}$, while for $\boldsymbol{q}$ parallel to the [111] direction $\beta = (2/3^{1/2})\beta_{14}$ for waves which induce the longitudinal electric field. The change in the sound velocity due to the interaction between the acoustic waves and conduction electrons is also related to the longitudinal conductivity σ_{zz} by

$$\frac{\Delta v_s}{v_s} = (2\pi/d\varepsilon v_s^2)[\beta^2 + (C\omega\varepsilon/4\pi e v_s)^2]\,\mathrm{Re}[1 - (4\pi\sigma_{zz}/\mathrm{i}\omega\varepsilon)]^{-1}. \tag{22}$$

As a numerical example, we shall consider the propagation of acoustic waves in n-InSb for a simple case with a constant relaxation time due to the scattering. The relevant values of physical parameters for n-InSb are (Nill and McWhorter 1966, Sutherland and Spector 1978, Wu and Tsai 1980): $n_0 = 1.75 \times 10^{14}\ \mathrm{cm}^{-3}$, $m^* = 0.013\, m_0$ (m_0 is the mass of a free electron), $\varepsilon = 18$, $\beta_{14} = 1.8 \times 10^4\ \mathrm{esu\ cm}^{-2}$, $C = 4.5\ \mathrm{eV}$, $E_g = 0.2\ \mathrm{eV}$, $d = 5.8\ \mathrm{g\ cm}^{-3}$, $\tau = 10^{-12}\ \mathrm{s}$ and $v_s = 4 \times 10^5\ \mathrm{cm\ s}^{-1}$. We plot the absorption coefficient $\alpha_\parallel$ as a function of sound frequency at $T = 4.2\ \mathrm{K}$ and $B = 3\ \mathrm{kG}$ as shown in figure 1. It can be seen that the absorption coefficient increases rapidly with the sound frequency up to about $\omega = 1.3 \times 10^{11}\ \mathrm{rad\ s}^{-1}$ and then decreases with the sound frequency. This is the same as our previous results (Wu and Tsai 1980) or the result for n-GaAs (Jacoboni

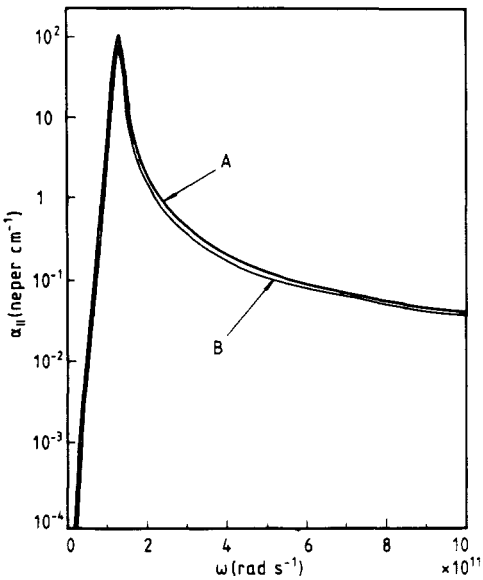

Figure 1. Absorption coefficient α as a function of frequency ω in n-InSb at $B = 3$ kG and $T = 4.2$ K. A, q parallel to [111]; B, q parallel to [110].

and Prohofsky 1969) except the maximum point becomes quite a sharp cusp in the present result. In figure 2, the change in sound velocity is plotted as a function of sound frequency at $T = 4.2$ K and $B = 3$ kG. It shows that in the low-frequency region the negative value of the change in sound velocity, $-\Delta v_s/v_s$, increases with the sound frequency and then drops rapidly to zero at about $\omega = 1.3 \times 10^{11}$ rad s^{-1}. After $\omega = 1.3 \times 10^{11}$ rad s^{-1}, the positive value of the change in sound velocity, $\Delta v_s/v_s$, increases

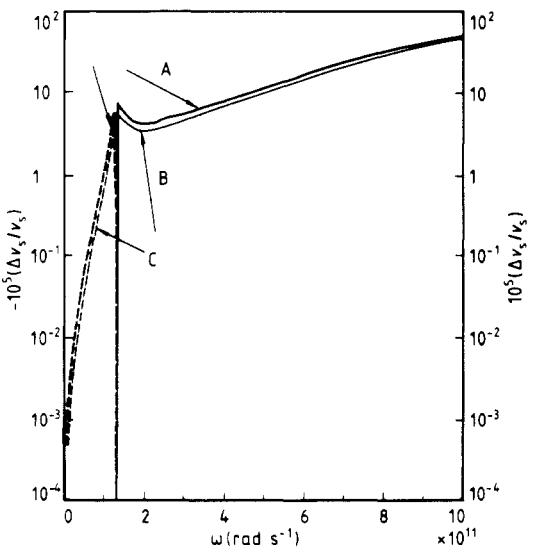

Figure 2. Change in sound velocity $\Delta v_s/v_s$ as a function of frequency ω in n-InSb at $B = 3$ kG and $T = 4.2$ K. Full curves, positive values of $\Delta v_s/v_s$; broken curves, negative values of $\Delta v_s/v_s$. A, q parallel to [111]; B, C, q parallel to [110].

rapidly with sound frequency to a local cusp-like maximum and then decreases to a local minimum. From $\omega = 2 \times 10^{11}$ rad s^{-1} the change in sound velocity $\Delta v_s/v_s$ increases monotonically with the sound frequency. Hence the sound frequency will influence the sound velocity in solids quite considerably. In order to study this property in more detail, we plotted the absorption coefficient and change in sound velocity as a function of the DC magnetic field at $T = 4.2$ K as shown in figure 3. It is found that the absorption coefficient decreases quite slowly with the DC magnetic field up to about $B = 100$ kG and then increases slowly with field at $\omega = 5 \times 10^{10}$ rad s^{-1} as shown in figure 3(a). However, at $\omega = 10^{11}$ rad s^{-1} as shown in figure 3(b), the absorption coefficient decreases monotonically with the magnetic field. And when the sound frequency goes up to $\omega = 5 \times 10^{11}$ rad s^{-1} as shown in figure 3(c), the absorption coefficient increases mon-

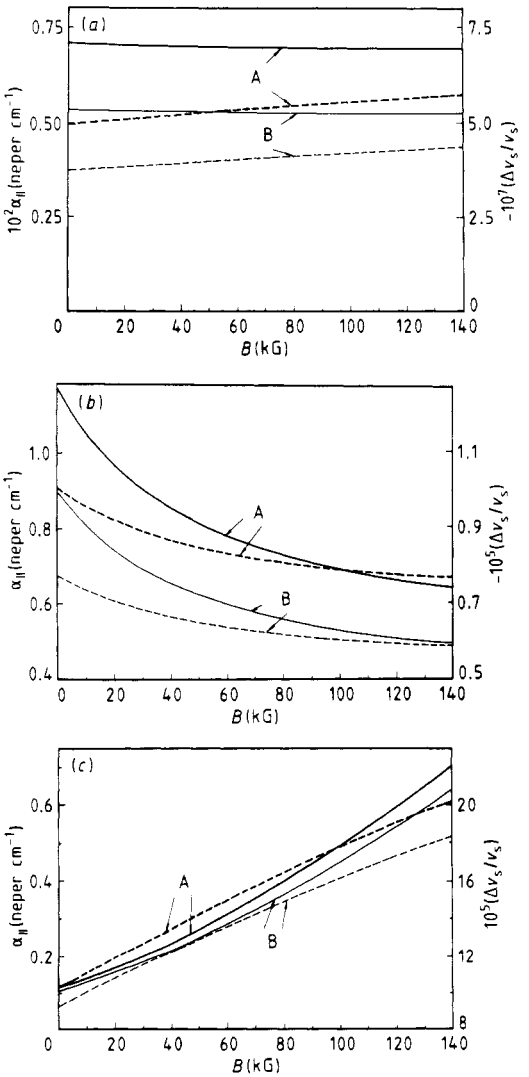

Figure 3. Absorption coefficient α (full curves) and change in sound velocity $\Delta v_s/v_s$ (broken curves) as a function of DC magnetic field B in n-InSb at $T = 4.2$ K for (a) $\omega = 5 \times 10^{10}$ rad s^{-1}; (b) $\omega = 10^{11}$ rad s^{-1}; (c) $\omega = 5 \times 10^{11}$ rad s^{-1}. A, q parallel to [111]; B, q parallel to [110].

otonically with the magnetic field. We can also see that the sound velocity decreases with the magnetic field from a value less than $v_s = 4 \times 10^5$ cm s^{-1} at $\omega = 5 \times 10^{10}$ rad s^{-1}. When the sound frequency is at $\omega = 10^{11}$ rad s^{-1}, the sound velocity increases with the magnetic field from the sound velocity less than $v_s = 4 \times 10^5$ cm s^{-1}. As the sound frequency is going up to $\omega = 5 \times 10^{11}$ rad s^{-1}, the sound velocity increases with the magnetic field from the sound velocity being larger than 4×10^5 cm s^{-1}, thus the change in sound velocity becomes positive in the higher frequency region. Figure 4 shows the absorption coefficient and change in sound velocity as a function of the DC magnetic field at $T = 19.7$ K. It is found that as the sound frequency is at $\omega = 5 \times 10^{10}$ rad s^{-1} the absorption coefficient decreases monotonically with the magnetic field and the sound velocity increases monotonically with the magnetic field when the sound velocity is inside

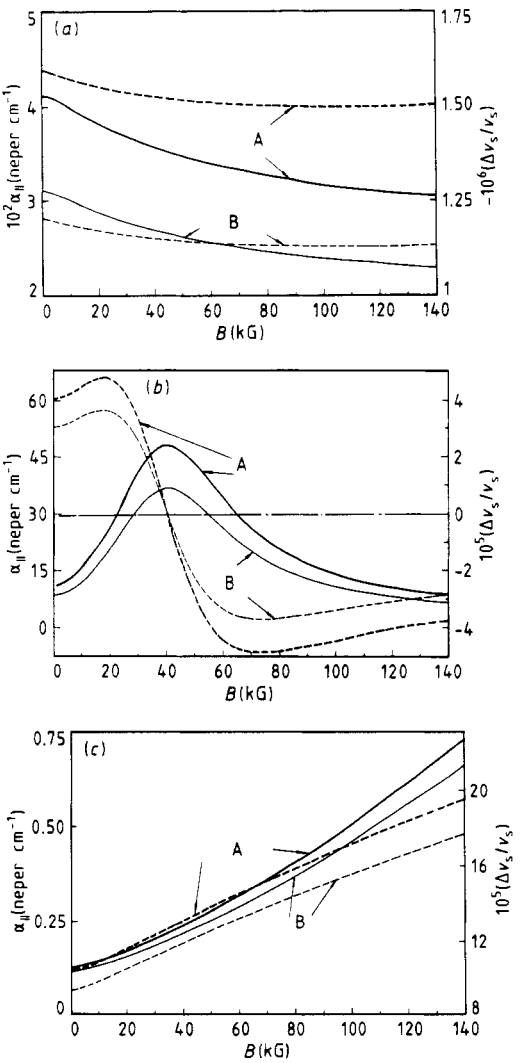

Figure 4. Absorption coefficient $\alpha_{\parallel}$ (full curves) and change in sound velocity $\Delta v_s/v_s$ (broken curves) as a function of DC magnetic field B in n-InSb at $T = 19.7$ K for (*a*) $\omega = 5 \times 10^{10}$ rad s^{-1}; (*b*) $\omega = 10^{11}$ rad s^{-1}; (*c*) $\omega = 5 \times 10^{11}$ rad s^{-1}. A, q parallel to [111]; B, q parallel to [110].

4×10^5 cm s^{-1}. However, when the sound frequency is at 10^{11} rad s^{-1}, the absorption coefficient changes quite considerably with the magnetic field, and there is a maximum value at $B = 40$ kG. Moreover, the change in sound velocity will change quite considerably with the magnetic field for the sound velocity being larger than 4×10^5 cm s^{-1}. We can see that there exist one maximum and one minimum in the change of sound velocity with the magnetic field. Therefore the temperature will also influence the magneto-acoustic phenomena in semiconductors. When the sound frequency is at $\omega = 5 \times 10^{11}$ rad s^{-1}, both the absorption coefficient and change in sound velocity will increase monotonically with the magnetic field.

4. Discussion

From the numerical analysis presented here, it can be seen that the absorption coefficient and the change in sound velocity are abnormal when the sound frequency is at $\omega = 1.3 \times 10^{11}$ rad s^{-1}. When the sound frequency is below 1.3×10^{11} rad s^{-1} the absorption coefficient increases with the sound frequency and the sound velocity decreases with the sound frequency. However, when the sound frequency is larger than 1.3×10^{11} rad s^{-1}, the absorption coefficient decreases monotonically with the sound frequency and the sound velocity increases abruptly with the sound frequency from $v_s = 4 \times 10^5$ cm s^{-1}. This discontinuous point comes from introducing a constant relaxation time due to the electron scattering in solids at the lower frequency region. In the lower frequency region, the absorption coefficient decreases with the magnetic field and the sound velocity increases from a value below $v_s = 4 \times 10^5$ cm s^{-1}. However, when the sound frequency is large enough, the absorption coefficient and change in sound velocity increase monotonically with the magnetic field due to the non-parabolicity of energy band structure in semiconductors. Therefore the magneto-acoustic phenomena in semiconductors will be affected by the correction of the non-linear effect from the Heisenberg equation of motion and the electron relaxation time due to the scattering in semiconductors.

For comparison, the result for the longitudinal conductivity using the parabolic model can be expressed by

$$\begin{aligned}\sigma_{zz} = \frac{(\omega_p^*)^2(\theta E_g)^{1/2}}{4(2\pi)^{1/2}\,i\omega}\Bigg(W[i(\tfrac{1}{2}E_g\theta)^{1/2}] - \frac{q\hbar E_g^{3/2}}{4(m^*)^{1/2}A_q}\Bigg[\Bigg[\frac{q\hbar\theta}{m^*}(\tfrac{1}{4}q^2\hbar^2 + m^*E_g)^{1/2} \\ + i\left(\frac{q^2\hbar^2\theta}{2m^*} + 2(2 + E_g\theta) - \frac{4q^2\hbar^2(\frac{1}{4}q^2\hbar^2 + m^*E_g)}{m^{*2}A_q}\right)\Bigg] \\ \times W\{(\theta/2m^*)^{1/2}[\tfrac{1}{2}q\hbar + i(\tfrac{1}{4}q^2\hbar^2 + m^*E_g)^{1/2}]\} \\ + \Bigg[\frac{q\hbar\theta}{m^*}(\tfrac{1}{4}q^2\hbar^2 + m^*E_g)^{1/2} - i\left(\frac{q^2\hbar^2\theta}{2m^*} + 2(2 + E_g\theta)\right. \\ \left. - \frac{4q^2\hbar^2(\frac{1}{4}q^2\hbar^2 + m^*E_g)}{m^{*2}A_q}\right)\Bigg] W\{-(\theta/2m^*)^{1/2}[\tfrac{1}{2}q\hbar - i(\tfrac{1}{4}q^2\hbar^2 + m^*E_g)^{1/2}]\} \\ + \frac{4i\Omega^2\hbar^2}{A_q}\left\{W\left[(\theta/2m^*)^{1/2}\left(\tfrac{1}{2}q\hbar + \frac{\Omega m^*}{q}\right)\right]\right. \\ \left. - W\left[-(\theta/2m^*)^{1/2}\left(\tfrac{1}{2}q\hbar - \frac{\Omega m^*}{q}\right)\right]\right\}\Bigg]\Bigg)\end{aligned} \tag{23}$$

where

$$A_q = \Omega^2\hbar^2 + E_g q^2\hbar^2/m^* + (q^2\hbar^2/2m^*)^2. \tag{24}$$

It can be seen that σ_{zz} is independent of the DC magnetic field for the parabolic band structure if the electron relaxation time is not energy dependent. Thus, the absorption coefficient and change in sound velocity for the parabolic model is independent of the magnetic field with a constant relaxation time. However, if the electron relaxation time is energy dependent, then the absorption coefficient and change in sound velocity depend on the magnetic field. For the non-parabolic band structure, it can be seen that the absorption coefficient and change in sound velocity will depend on the magnetic field even with a constant electron relaxation time as we have shown in the last section, because the factor a_n plays an important role in strong magnetic fields. Moreover, if we also consider the energy-dependent relaxation time, the effect of non-parabolicity on the magneto-acoustic phenomena will demonstrate stronger magnetic-field dependence.

In our numerical analysis presented in the last section, we have assumed a constant electron relaxation time. However, an energy-dependent relaxation time can give rise to a stronger magnetic field dependence of the magneto-acoustic absorption in the longitudinal magnetic field. The energy-dependent relaxation times of the non-parabolic band structure for several fundamental scattering processes are given as follows (Smith 1969, Nag 1972):

(a) Acoustic phonon scattering

$$\tau = \tau(E_{kn}) = K_1 E_{kn}^{-1/2}\Theta_{kn}^{3/2} \tag{25a}$$

(b) Piezo-electric scattering

$$\tau = \tau(E_{kn}) = K_2 E_{kn}^{1/2}\Theta_{kn}^{1/2} \tag{25b}$$

(c) Ionised-impurity scattering

$$\tau = \tau(E_{kn}) = K_3 E_{kn}^{3/2}\Theta_{kn}^{-1/2} \tag{25c}$$

where K_1, K_2 and K_3 are constants.

In strong magnetic fields and at low temperatures, equations (25*a*)–(25*c*) can be approximated as follows:

(a) Acoustic phonon scattering

$$\tau \simeq K_1'[a_n^3(a_n - 1)]^{-1/2} \tag{26a}$$

(b) Piezo-electric scattering

$$\tau \simeq K_2'[a_n^{-1}(a_n - 1)]^{1/2} \tag{26b}$$

(c) Ionised-impurity scattering

$$\tau \simeq K_3'[(a_n(a_n - 1)^3]^{1/2} \tag{26c}$$

where K_1', K_2' and K_3' are constants. From equations (26*a*)–(26*c*), it is shown that τ is dependent on a_n for all these three types of scattering mechanisms in strong magnetic fields. This means that τ depends on the DC magnetic field. Consequently, if we are taking into account the energy-dependent relaxation time, the effect of non-parabolicity will influence quite considerably on the magneto-acoustic phenomena in semiconductors. Moreover, from equation (18), the relaxation time will vary from sample to

sample due to the effective mass of electrons m^* and the energy gap E_g. Therefore, the non-parabolicity of energy band structure and the energy-dependent relaxation time can be used to explain the Nill and McWhorter experimental results of (1966) in which the acoustic absorption coefficient depends on the longitudinal magnetic field.

The frequency range discussed in our present analysis might be difficult to observe with other types of phonon experiments. However, a technique for the monochromatic detection of 10^{12} Hz phonons is applied to the study of 20 cm^{-1} phonons in ruby (Anderson and Sabisky 1968). Other techniques for phonon spectroscopy are based on phonon-induced optical fluorescence (Renk and Deisenhofer 1971) or on changes in microwave absorption induced by phonon transitions (Shiren 1961). By applying external fields to the crystal it should be possible to realise tunable detectors for 10^{12} Hz phonons, thus extending the region of existing phonon spectrometers. Abe and Mikoshiba (1971) investigated the magneto-acoustic amplification in semiconductors in the frequency range from 10^9–10^{12} rad s^{-1}. Mosekilde (1974) studied the acousto-electric interaction of GaAs in the sound frequency range from 10^{11}–10^{13} rad s^{-1}. He showed that the acoustic gain factor appears in the range from 10^{11}–10^{12} rad s^{-1}. Hence, it seems possible to investigate the magneto-acoustic phenomena in semiconductors from 10^{10}–10^{12} rad s^{-1}.

Acknowledgment

This work was partially supported by the National Science Council of China.

References

Abe Y and Mikoshiba N 1971 *J. Appl. Phys.* **42** 190–9
Abramowitz M and Stegun I A 1964 *Handbook of Mathematical Functions* (Washington: National Bureau of Standards)
Anderson C H and Sabisky E S 1968 *Phys. Rev. Lett.* **21** 987–90
Aliev M I, Askerov B M, Agaeva R G, Daibov A Z and Ismailov I A 1974 *Fiz. Tekh. Poluprov.* **9** 570–2 (1975 *Sov. Phys.–Semicond.* **9** 377–8)
Broom R 1958 *Proc. Phys. Soc.* **71** 500
Eisenmenger W 1976 *Physical Acoustics* vol XII (New York: Academic) pp 79–153
Frederikse H P R and Hosler W R 1957 *Phys. Rev.* **108** 1136–45
Grill W and Weis O 1974 in *Microwave Acoustics* (London: Institute of Physics) p 179
Hansen O P 1981 *J. Phys. C: Solid State Phys.* **14** 5501–4
Jacoboni C and Prohofsky 1969 *J. Appl. Phys.* **40** 454–61
Lifshitz T M, Oleinikov A Ya and Shulman A Ya 1966 *Phys. Status Solidi* **14** 511–6
Mosekilde E 1974 *Phys. Rev.* B **9** 682–9
Nag B R 1972 *Theory of Electrical Transport in Semiconductors* (Oxford: Pergamon)
Nill K W and McWhorter A L 1966 *J. Phys. Soc. Japan Suppl.* **21** 755–9
Renk K F and Deisenhofer J 1971 *Phys. Rev. Lett.* **26** 764–6
Sharma S and Phadke U P 1972 *Phys. Rev. Lett.* **29** 272–4
Shiren N S 1961 *Phys. Rev. Lett.* **6** 168–70
Smith R A 1969 *Wave Mechanics of Crystalline Solids* (London: Chapman and Hall)
Smith W D, Miller J G, Sundfors R K and Bolef D I 1971 *J. Appl. Phys.* **42** 2579–84
Spector H N 1966 *Solid State Physics* **19** 291–361 (New York: Academic)
Sutherland F R and Spector H N 1978 *Phys. Rev.* **17** 2728–32; 2733–9
Whalen J J and Westgate C R 1972 *J. Appl. Phys.* **43** 1965–75
Wu C C and Tsai J 1972 *J. Phys. C: Solid State Phys.* **5** 2419–26
—— 1979 *Solid State Commun.* **32** 801–3
—— 1980 *J. Appl. Phys.* **51** 3751–5